REPORT

Cassini Ion and Neutral Mass Spectrometer: Enceladus Plume Composition and Structure

J. Hunter Waite Jr.,[1] Michael R. Combi,[1] Wing-Huen Ip,[2] Thomas E. Cravens,[3] Ralph L. McNutt Jr.,[4] Wayne Kasprzak,[5] Roger Yelle,[6] Janet Luhmann,[7] Hasso Niemann,[5] David Gell,[1] Brian Magee,[1] Greg Fletcher,[1] Jonathan Lunine,[6,8] Wei-Ling Tseng[2]

The Cassini spacecraft passed within 168.2 kilometers of the surface above the southern hemisphere at 19:55:22 universal time coordinated on 14 July 2005 during its closest approach to Enceladus. Before and after this time, a substantial atmospheric plume and coma were observed, detectable in the Ion and Neutral Mass Spectrometer (INMS) data set out to a distance of over 4000 kilometers from Enceladus. INMS data indicate that the atmospheric plume and coma are dominated by water, with significant amounts of carbon dioxide, an unidentified species with a mass-to-charge ratio of 28 daltons (either carbon monoxide or molecular nitrogen), and methane. Trace quantities (<1%) of acetylene and propane also appear to be present. Ammonia is present at a level that does not exceed 0.5%. The radial and angular distributions of the gas density near the closest approach, as well as other independent evidence, suggest a significant contribution to the plume from a source centered near the south polar cap, as distinct from a separately measured more uniform and possibly global source observed on the outbound leg of the flyby.

The INMS instrument on the Cassini spacecraft, pointing within 60° of the direction of motion of the spacecraft and traveling with a relative velocity of ~8 km s^{-1} to Enceladus, was able for the first time to investigate the composition and spatial distribution of gases in the plume and coma surrounding Enceladus (Fig. 1). Previous close flybys of Enceladus (<4000 km) by the Cassini spacecraft have all been carried out with INMS pointed in the anti-ram direction of motion of the spacecraft, thereby precluding possible measurements of any neutral gases associated with Enceladus.

The Cassini INMS is a dual–ion source quadrupole mass spectrometer covering the mass-to-charge ranges 0.5 to 8.5 and 11.5 to 99.5 daltons (*1*, *2*). The dual-source design combines classic closed– and open–ionization source configurations that measure inert species and reactive species and ions, respectively. The primary data reported in this paper were obtained with the closed source. In the closed source, the neutral gas flows into a spherical antechamber where it thermally accommodates with the walls before flowing through a transfer tube to an electron ionization source and is ionized by electron impact at 70 eV. The high flyby velocity of the Cassini spacecraft with respect to Enceladus (~8 km s^{-1}) produces a dynamic pressure enhancement in the antechamber that increases sensitivity (*1*, *2*), but at a reduced level because of the 60° orientation of the sensor with respect to the ram direction of the spacecraft's motion.

The spectrum displayed in Fig. 2 indicates a mass scan covering the range 1 to 99 daltons. The individual mass spectra that were used to form the spectrum were acquired every 4.6 s for the time period when the spacecraft was closer than 500 km to the surface of Enceladus. The spectra have been added to enhance the signal-to-noise ratio. The background subtraction for ingress and egress data are treated separately to account for changes observed well before and well after the Enceladus flyby. The primary constituents H_2O, CO_2, N_2 or CO, and CH_4 are evident from the primary mass peaks at 18, 44, 28, and 16 daltons, respectively. Mass peaks are also measured for the minor atmospheric species (C_2H_2 and C_3H_8). Other species that could be present at a level <0.5% include NH_3 and HCN.

The responses of all of the measurable product channels of the primary constituents of interest were determined during the flight unit and engineering unit calibrations (with the exception of H_2O, NH_3, and HCN, which were obtained from National Institute of Standards and Technology tabulations). These responses were subsequently used in the deconvolution of the spectra. Because of the nature of the electron-beam ionization source, the signal in each mass bin is a combination of the signals from the ionization or dissociative ionization of several constituents. Spacecraft velocity and attitude are used to compute the ram flow enhancement. From these data, a matrix is constructed relating instrumental response for various mass channels to the atmospheric composition. Inversion of this matrix with suitable numerical methods (*3*) yields abundances for a range of constituents. The measurements (and matrix elements) are weighted by the reciprocal measurement error.

The best fit to the atmospheric composition based on the mass deconvolution (according to a reduced chi-squared metric) gives 91 ± 3% H_2O, 3.2 ± 0.6% CO_2, 4 ± 1% N_2 or CO (depending on the identity of the mass peak at 28 daltons), and 1.6 ± 0.4% CH_4, where the error estimates are the larger of the fit range or the 1σ statistical error of the fit and do not include systematic errors from factors such as calibration, which may be as high as 20% (Table 1). Statistically meaningful residuals in the mass ranges 14 to 17 and 26 to 27 daltons suggest that there may also be trace quantities (<~1%) of ammonia, acetylene, hydrogen cyanide, and propane.

The signal-to-noise ratio in the mass-18 channel (predominantly the H_2O signature) is sufficient within 4000 km of Enceladus to investigate how the water vapor density varies along the track of the spacecraft (Fig. 3). In Fig. 3, we also compare the water vapor density with the density of dust particles greater than 2 μm in size inferred from the Cassini Cosmic Dust Analyzer (CDA) (*4*). There is noticeable asymmetry with respect to the closest approach in both data sets and a reasonable correlation between them, but with an offset of 32 s. Furthermore, water vapor density variations well above the level of expected statistical variation suggest spatial and/or temporal structure of the outgassing source. Moreover, the spatial variability and the asymmetry of the water vapor and dust distributions with respect to closest approach (Fig. 3) suggest an association with the southern thermal hot spot (*5*, *6*).

The mass spectrum obtained by INMS can be used to understand the origin and evolution of the interior of Enceladus. The inferred surface pressure of the atmosphere (properly an exosphere) lies between 10^{-1} and 10^{-4} nanobars, such that collisions and subsequent gas-phase chemical reactions play a minor role within the atmospheric plume. Furthermore, the ionization and dissociation time constants (hours at a

[1]Department of Atmospheric, Oceanic, and Space Sciences, University of Michigan, Ann Arbor, MI 48109, USA. [2]Institutes of Astronomy and Space Science, National Central University, Chung Li 32054, Taiwan. [3]Department of Physics and Astronomy, University of Kansas, Lawrence, KS 66045, USA. [4]Applied Physics Laboratory, Johns Hopkins University, Laurel, MD 20723, USA. [5]NASA Goddard Space Flight Center, Greenbelt, MD 20771, USA. [6]Lunar and Planetary Laboratory, University of Arizona, Tucson, AZ 85721, USA. [7]Space Science Laboratory, University of California, Berkeley, CA 94720, USA. [8]Istituto di Fisica dello Spazio Interplanetario, Via del Fosso del Cavaliere 100, 00133 Rome, Italy.

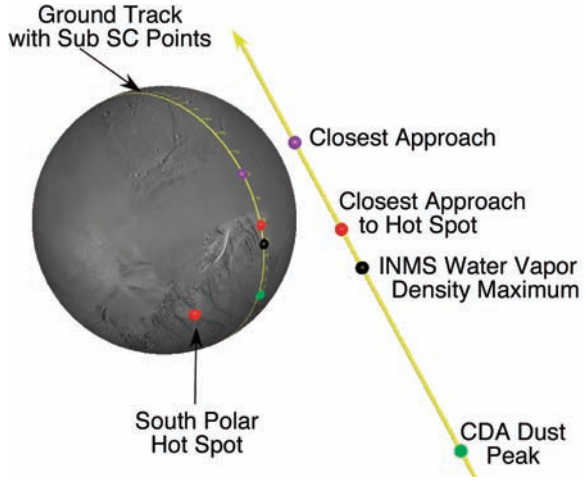

Fig. 1. View of Enceladus showing surface features and the Cassini ground track during the flyby on 14 July 2005. The south polar hot spot is shown in red, amidst the surface feature known as the tiger stripes. The spacecraft trajectory is shown in yellow. The colors of the points along the trajectory represent Cassini's closest approach to Enceladus (purple), the closest approach to the southern polar hot spot (red), the point along the track where INMS saw the maximum water vapor density (black), and the point along the track where the CDA saw the peak in dust particle density (green). The direction of motion of the spacecraft (ram direction) is represented by the arrowhead on the trajectory. SC, spacecraft.

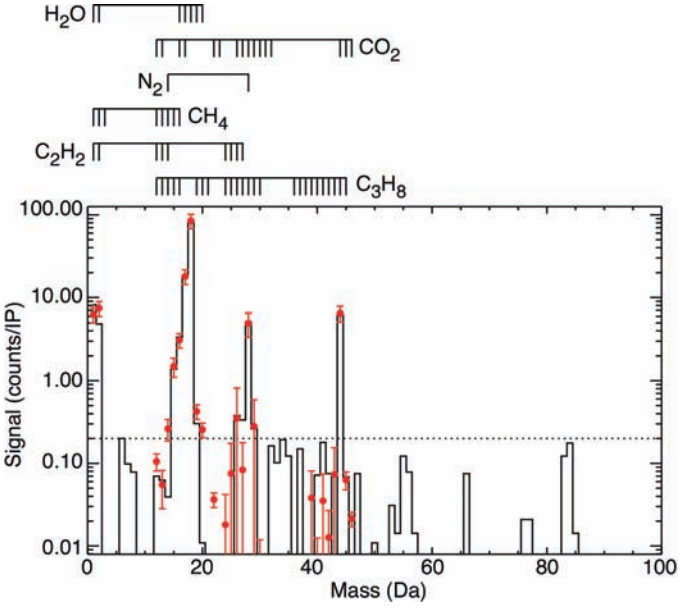

Fig. 2. Average mass spectrum for altitudes below 500 km. The solid black line indicates the measured average spectrum and the red symbols represent the reconstructed spectrum. The error bars displayed are the larger of the 20% calibration uncertainty or the 1σ statistical uncertainty. The dotted line is indicative of the 1σ noise level. The dissociative ionization products produced by the electron ionization source for each constituent are shown above the figure. Da, daltons; IP, integration period.

Table 1. Composition of the gas plume and coma associated with Enceladus. The minimum and maximum values represent the range of values associated with adopting different compositional mixtures. The standard deviation represents the largest statistical uncertainty associated with the fit of each constituent.

Species	Minimum	Maximum	SD
H_2O	0.9070	0.9150	0.0300
CO_2	0.0314	0.0326	0.0060
Mass 28 (CO or N_2)	0.0329	0.0427	0.0100
CH_4	0.0163	0.0168	0.0040

minimum) are orders of magnitude longer than the inferred transport time from the surface to the point of measurement (~6 min). Therefore, the outgassing products measured by INMS are presumed to have been produced in aqueous and/or solid phases or in a high-pressure gas channel within Enceladus before outgassing or sputtering took place. Furthermore, the nonspherical density variations of the plume and coma suggest that the observed composition is an accurate representation of the gas composition that occurs at the site of local outgassing from the south polar hot spot (Table 1). This suggestion of a close association between surface and plume composition is reinforced by the strong correlation between the surface composition derived from data collected by the Cassini Visual and Infrared Mapping Spectrometer (VIMS) within the tiger stripes associated with the south polar hot spot (*7*) and the plume composition measured by INMS 250 km above the boundary of the south polar region (*6*). VIMS measured predominantly water ice, with an admixture of carbon dioxide (very similar to the findings of INMS), and an organic signature from a light hydrocarbon. Furthermore, from the VIMS data we infer an upper limit for a CO mixing ratio of 0.5% (*8*). Similarly, the Cassini Ultraviolet Imaging Spectrograph (UVIS) observations set an upper limit of 2% for the CO mixing ratio (*9*, *10*). When considered together, the VIMS and UVIS observations suggest, although not conclusively, that the INMS peak at mass 28 is most likely produced by N_2. Follow-up observations are needed to verify this.

The presence of N_2 and little, if any, NH_3 (<0.5%) is notable, because ever since the discovery of large crater-free areas on Enceladus by Voyager imaging, ammonia has been a preferred substance for lowering the melting point of water ice and increasing its buoyancy so as to aid or enable resurfacing (*11*). Ammonia was reported to have been detected as a very weak hydrate feature in one ground-based near-infrared spectroscopic observation of Enceladus (*12*) but not in another (*13*). Our failure to detect ammonia suggests either that it is not involved in the subsurface mechanisms that created the plume or that aqueous chemistry within the interior source regions of the plume effectively converts NH_3 to N_2 before it can be exposed to or ejected from the surface. We can, however, virtually rule out chemical complexing of some or all of the NH_3 with the walls of the INMS antechamber, a phenomenon seen in laboratory studies of ammonia (*14*) but unlikely here on the basis of our careful analysis of the background changes after the flyby. With respect to the identification of the molecular nitrogen, we cannot completely rule out the mass-28 species being CO rather than N_2, in which case the outgassing observed from the plume would have a composition that is remarkably close to that of comets, as inferred from multiple cometary observations [tables 1 and 2 in (*15*)]. Thus, further study both of the identity of the mass-28 peak and of possible loss mechanisms that might make NH_3 difficult to observe are warranted.

The radial and angular density distributions of water vapor are also important in understanding the nature of the processes responsible for the outgassing. The fit to the functional form natural log (density) versus 1/(distance to the center of Enceladus)^x for the combined ingress and egress data set gives a best fit of x = 1.5 ± 0.1 (supporting online material text). However, asymmetries in this fit inbound (x = 2.0) versus outbound (x = 1.1) and irregularities near the closest approach, as well as evidence from other Cassini investigations (*4*–*7*, *10*), suggest an asymmetric gas distribution organized around a source centered near the "warm" (*5*, *6*) south polar cap. To understand this asymmetry, we used a direct-simulation Monte Carlo model developed originally for comets (*16*, *17*) to

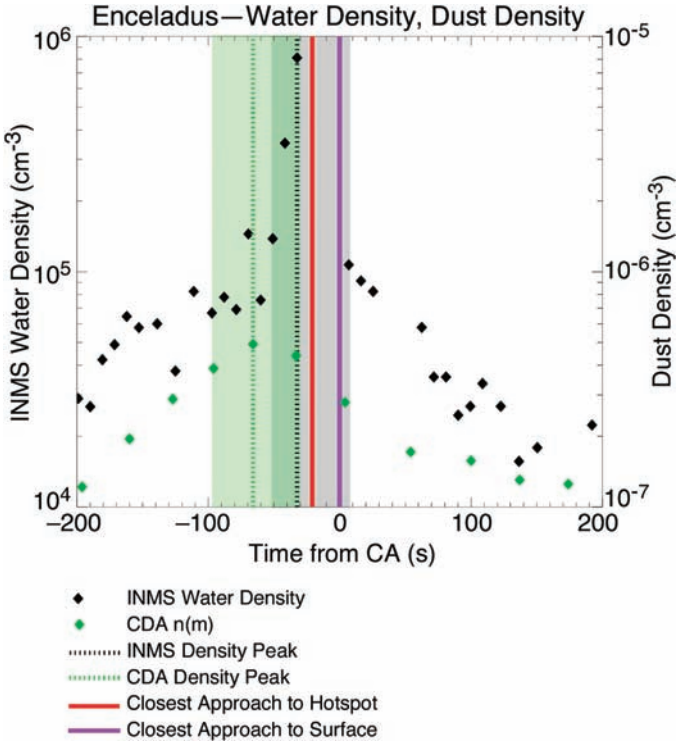

Fig. 3. Plot of the INMS water density and CDA dust density as a function of time along the orbital trajectory. CDA measurements represent particles larger than 2 μm in grain size. Shifting the INMS density data −32 s from the closest approach (CA) maximizes the Pearson correlation coefficient (~0.85) between INMS-derived water densities and CDA-derived dust densities. The light green shading indicates the estimated timing uncertainty in the dust peak, the gray shading indicates the estimated uncertainty in the water vapor peak, and the dark green shading indicates the overlap.

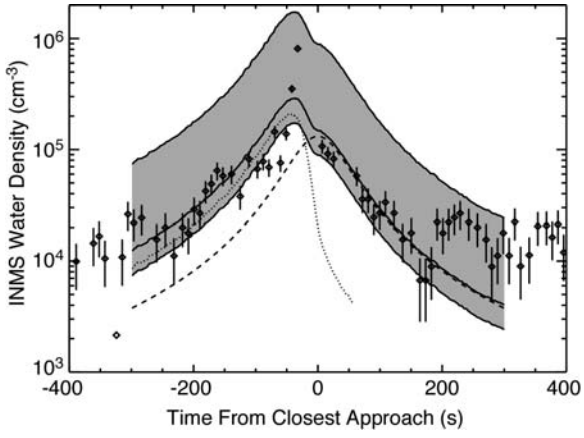

Fig. 4. Comparison of model results to INMS density data near its closest approach to Enceladus. The diamonds show the INMS-measured water density with the 1σ uncertainties indicated by the vertical lines. The dotted line corresponds to the south polar source model covering latitudes from −90° to −82°. The dashed line corresponds to a spherical global, possibly sputtered source. The solid line corresponds to the sum of these two sources. The gray area denotes the density range.

which we have added the effect of the weak gravitational field. The water molecules are introduced into the model from (*5*, *6*) the south polar source and (*1*) a uniform surface (possibly sputtering) source. Several source characterizations were attempted, varying the relative upward speed from the source at the surface, the size of the south polar source (4° to 15° from the pole), the temperature, and the source strengths. The uniform source is a simple spherical outflow model with a density of $n = S/(4\pi v R_E^2)$, where S is the total global source rate, v is the average upward molecular velocity, and R_E is the distance from the center of Enceladus.

Figure 4 shows the results of modeling the INMS response to the plume and coma of Enceladus in the time period of 400 s before and after the closest approach, which corresponds to 1700 km from the center of Enceladus. The source rate from the model's uniform component (the dashed line) is $S_1 \approx 1.2 \times 10^{26}$ molecules s^{-1}, assuming a speed of about 400 m s^{-1}. The model's south polar plume extends to a latitude of −82° and has a thermal speed distribution for the water sublimation temperature of 190 K and a source rate of $S_2 \approx 1.7 \times 10^{26}$ molecules s^{-1} (*18*). Varying the temperature from 140 K (average temperature of the tiger stripes region) to 270 K (suggested in some subsurface heating scenarios) introduces a range of 20% to the source strength. A small third "jet" source with a half-cone angle width of 3° and a source strength of only $\sim 5 \times 10^{23}$ molecules s^{-1} could explain the peak; however, the deviation of these two points from the model is of the same magnitude as several other points and may simply result from temporal or spatial irregularities in the emission from the surface. The total H_2O production rate from Enceladus ($S = S_1 + S_2$) is $S \approx 1.5 \times 10^{26}$ to 4.5×10^{26} molecules s^{-1}, and the total gas production rate $S_{gas} \approx 1.7 \times 10^{26}$ to 5.0×10^{26} molecules s^{-1}, assuming the gas is 90% H_2O from INMS measurements.

The INMS measurements corresponding to egress times larger than 250 s after the closest approach show an extended plateau that does not continue the downward trend of the models. The region within 2000 km from the center of Enceladus only takes about 1 to 2 hours to populate. If these larger values in the extended region are caused by temporal variations in the source rate of water from Enceladus, as has been seen in Cassini UVIS measurements of atomic oxygen (*19*), then source rates up to a factor of 6 or more than the modeled values could occur. The lower INMS measurements (compared with the nominal model in Fig. 4) indicate source rates of a factor of 0.6 below the nominal model values. The bounds of the minimum and maximum model indicate a highly variable source rate that varies on time scales of less than 1 hour over a wide range from 1×10^{26} s^{-1} to 3×10^{27} s^{-1}. The density range is shown as the broad gray area in Fig. 4. The larger values in this range are more indicative of the broad distribution seen at large distances from Enceladus and are comparable to the source rates required to account for the water source of OH in the whole circumsaturnian region. The density peak seen near the closest approach could result from the start of a new high–source rate episode. Notably, the high level and irregularity of the source rate indicated by the egress data, 250 to 400 s after the closest approach, are far to the north and cannot be traced directly back to the south polar plume. Therefore, it is likely that the south polar plume and the uniform source are both highly variable.

The special role of Enceladus in supplying water vapor and its related neutral and ionized constituents to the magnetosphere of Saturn has been recognized since the observations by the Hubble Space Telescope (HST) of a substantial OH torus (*20*). These results led to model-based estimates of the source strengths of the various icy moons and rings necessary to reproduce the observed spatial variations. In particular, Jurac *et al.* (*21*) concluded that about 80% of the required water vapor must come from Enceladus and the E-ring region, implying that the production from Enceladus was $\sim 3.75 \times 10^{27}$ molecules s^{-1} or 93 kg s^{-1}, which could be consistent with the higher set of INMS measurements at larger radial distances (~2000 km), especially after the closest approach. This could mean that the water source rate from

Enceladus might vary markedly by nearly an order of magnitude on time scales of hours (*19*). Jurac *et al*. (*21*) also suggested that impacts by E-ring particles, a possible source, would be insufficient to produce this amount. Nevertheless, Roddier *et al*. (*22*) had imaged a transient feature with HST that could have been interpreted as a large, impact-produced vapor cloud. The fresh deposits on Enceladus' surface suggested by its high albedo also reinforced the idea that E-ring grains are constantly being swept up, along with any larger objects that may be present. Sputtering of ice by energetic O^+ ions as a source required more surface area than could be accounted for by the combination of Enceladus and the expected E-ring grains. In a subsequent paper, Jurac and Richardson (*23*) concluded that the source rate for the observed water needed to be three times larger and that its production mechanism remained unclear. The discovery by Cassini of an unexpected venting of water vapor from the south pole of Enceladus, of approximately the right amount, may provide a solution to this mystery.

References and Notes

1. J. H. Waite *et al.*, *Space Sci. Rev.* **114**, 113 (2005).
2. W. K. Kasprzak *et al.*, *Proc. SPIE* **2803**, 129 (1996).
3. W. H. Press, B. P. Flannery, S. A. Teukolsky, W. T. Vetterling, *Numerical Recipies* (Cambridge Univ. Press, Cambridge, 1986).
4. F. Spahn *et al.*, *Science* **311**, 1416 (2006).
5. J. R. Spencer *et al.*, *Science* **311**, 1401 (2006).
6. C. C. Porco *et al.*, *Science* **311**, 1393 (2006).
7. R. H. Brown *et al.*, *Science* **311**, 1425 (2006).
8. The VIMS-derived mixing ratio is based on the absence of CO absorption features in the gas column between the surface above the south polar cap and the spacecraft (10^{14} cm^{-2}), divided by the column density of water acquired by UVIS during a stellar occultation (1.5×10^{16} cm^{-2}) (*10*).
9. The absence of CO ultraviolet absorption bands in the UVIS occultation data sets an upper limit for CO abundance at 2% of the water density for a measured water column of 1.5×10^{16} cm^{-2} (*10*).
10. C. J. Hansen *et al.*, *Science* **311**, 1422 (2006).
11. S. W. Squyres, R. T. Reynolds, P. M. Cassen, S. J. Peale, *Icarus* **53**, 319 (1983).
12. J. P. Emery, D. M. Burr, D. P. Cruikshank, R. H. Brown, J. B. Dalton, *Astron. Astrophys.* **435**, 353 (2005).
13. D. P. Cruikshank *et al.*, *Icarus* **175**, 268 (2005).
14. S. Boone, M. F. Nicol, in *LPSC 21 Proc*. (Lunar and Planetary Institute, Houston, TX, 1991), pp. 603–610.
15. D. C. Bockelee-Morvan, J. Crovisier, M. J. Mumma, H. A. Weaver, in *Comets II*, M. C. Festou, H. U. Keller, H. A. Weaver, Eds. (Univ. Arizona Press, Tucson, AZ, 2004), pp. 391–423.
16. The observed asymmetries and the coincidence of water vapor, CO_2, and dust appearing to emanate from the south polar tiger stripes region of Enceladus indicate a possible cometary activity analog. Our analysis of the composition and plume shape suggests the temperature below the surface at the source of the water vapor must be somewhere in the range of at least ~190 to 273 K, the temperatures required for the sublimation of ice. If dust particles have been ejected from the cracks in the surface by the action of the flow of water molecules, then it is likely that the confined volume below the surface must be rather small so as to yield sufficiently high gas densities to achieve substantial dust entrainment (*24*). If the observed dust particles are ice condensates from the gas plumes emanating from the cracks, as has also been suggested for comets (*25*), then gas densities must also be quite high. In an expanding cometary coma, the number density of water molecules in which dust is effectively accelerated by the gas flow is greater than about 10^8 cm^{-3}. Near the nucleus, where the dust acceleration is the largest, gas densities are larger than 10^{11} cm^{-3} for a moderately bright comet like 1P/Halley or 1996 B2 (Hyakutake) (*25*). Taken together, this implies that the water flow exits from relatively small fissures in the surface [such as the tiger stripes (2 by 120 km) (*6*) themselves compared with the size of the general emitting region] and that the flow is already accelerated to rather large speeds and is correspondingly cooled below the reservoir temperature [in excess of 190 K (*26*)] when it passes through the surface. The fissures must also be large enough to allow at least semicollisional gas flow below the surface (i.e., the fissure's bore size must be larger than the mean free path between molecules). If the fissures are too small, then molecules will stick to the cold surfaces and never exit, sealing off the crack. Even the average temperature observed by the Composite Infrared Spectrometer of 140 K is far below the sublimation temperature so that most molecules striking the surface would stick. Such recondensation is a common feature included in porous subsurface cometary nucleus models (*27*).
17. M. R. Combi, *Icarus* **123**, 207 (1996).
18. The source strength inferred from the model allows us to estimate a surface density that can be compared to the UVIS observations (*10*) if we assume a thermal escape speed and an area of the outgassing. ISS (*6*) indicates that the tiger stripes region of ice crystal and dust generation presents 1 to 3% of the area of the polar cap at southern latitudes greater than 82°. If we assume that the gas production and dust and ice generation regions coincide, and if we further assume a thermal speed for the water vapor of 400 m s^{-1}, we derive an inferred near-surface density based on the extended plume measured by INMS of 1×10^9 to 5×10^9 cm^{-3}. On the other hand, UVIS (*10*) reports a water column density of 1.5×10^{16} cm^{-2} and infers a scale length of 80 km, which leads to a near-surface density of 1.9×10^9 cm^{-3}. This value is within the range inferred by INMS.
19. L. W. Esposito *et al.*, *Science* **307**, 1251 (2005).
20. D. E. Shemansky, P. Matherson, D. T. Hall, T. M. Tripp, *Nature* **363**, 329 (1993).
21. S. Jurac *et al.*, *Geophys. Res. Lett.* **29**, 2172 (2002).
22. C. Roddier, F. Roddier, J. E. Graves, M. J. Northcott, *Icarus* **136**, 50 (1998).
23. S. Jurac, J. D. Richardson, *J. Geophys. Res*. **110**, 10.1029/2004JA010635 (2005).
24. R. V. Yelle, L. A. Soderblom, J. R. Jokipii, *Icarus* **167**, 30 (2004).
25. T. Yamamoto, O. Ashihara, *Astron. Astrophys.* **152**, L17 (1985).
26. M. R. Combi, W. M. Harris, W. H. Smyth, in *Comets II*, M. C. Festou, H. U. Keller, H. A. Weaver, Eds. (Univ. Arizona Press, Tucson, AZ, 2004), pp. 523–552.
27. B. Davidsson, Y. Skorov, *Icarus* **168**, 163 (2004).

28. The Cassini INMS investigation is supported by contract number 1228303 from the NASA Jet Propulsion Laboratory. M.R.C. was supported by grant NAG5-12822 from the NASA Planetary Atmospheres Program. W.-H.I. was supported by grant NSC 94-2111-M-008-033.

Supporting Online Material

www.sciencemag.org/cgi/content/full/311/5766/1419/DC1
SOM Text
Fig. S1
Table S1

12 October 2005; accepted 12 December 2005
10.1126/science.1121290

REPORT

Enceladus' Water Vapor Plume

Candice J. Hansen,[1]* L. Esposito,[2] A. I. F. Stewart,[2] J. Colwell,[2] A. Hendrix,[1] W. Pryor,[4] D. Shemansky,[3] R. West[1]

The Cassini spacecraft flew close to Saturn's small moon Enceladus three times in 2005. Cassini's UltraViolet Imaging Spectrograph observed stellar occultations on two flybys and confirmed the existence, composition, and regionally confined nature of a water vapor plume in the south polar region of Enceladus. This plume provides an adequate amount of water to resupply losses from Saturn's E ring and to be the dominant source of the neutral OH and atomic oxygen that fill the Saturnian system.

The youthful geologic appearance of Enceladus (*1*) and the correlation of the peak density of Saturn's E ring with the orbit of Enceladus (*2*) have long led scientists to speculate that Enceladus is the source of the ring (*2*–*5*). The narrow size distribution of particles in the E ring suggests a liquid or vapor origin, in contrast to the broad range of particle sizes that would be generated by impacts (*2*). To test the hypothesis that Enceladus has geologic activity supplying the E ring as well as neutral species in Saturn's magnetosphere, the Cassini Ultraviolet Imaging Spectrograph (UVIS) team planned stellar occultation observations on Cassini's first and third close flybys of Enceladus to search for the presence of a tenuous atmosphere (*6*). The detection, by the Cassini Magnetometer team (*7*), of draped field lines consistent with the presence of an atmosphere gave further impetus to the second occultation observation. Because of Enceladus' small size and weak gravity (~12 cm/s^2), any sputtered or sublimated atmosphere will be lost (*8*); thus, if a tenuous atmosphere were to be detected, it would have to come from some sort of geologic activity. We now know that

[1]Jet Propulsion Laboratory/California Institute of Technology, 4800 Oak Grove Drive, Pasadena, CA 91109, USA. [2]Laboratory for Air and Space Physics (LASP), University of Colorado, Boulder, CO 80303, USA. [3]Space Environment Technologies, 320 North Halstead, Suite 170, Pasadena, CA 91107, USA. [4]Central Arizona College, Coolidge, AZ 85228, USA.

*To whom correspondence should be addressed. E-mail: Candice.j.Hansen@jpl.nasa.gov